Electronic Journal of Differential Equations, Vol. 2020 (2020), No. 70, pp. 1–23.
ISSN: 1072-6691. URL: http://ejde.math.txstate.edu or http://ejde.math.unt.edu

OPTIMAL CONTROL ANALYSIS APPLIED TO A TWO-PATCH MODEL FOR GUINEA WORM DISEASE

STEADY MUSHAYABASA, ANTHONY A. E. LOSIO,
CHAIRAT MODNAK, JIN WANG

Communicated by Suzanne M. Lenhart

Abstract. We applied optimal control theory to a mathematical model for guinea worm disease, to determine the effectiveness of optimal education campaigns on long-term dynamics of the disease. Our model is concerned with two different host populations, represented by two patches, sharing a common water source. We computed the basic reproduction number of the model and demonstrated that whenever the reproduction number is less than unity the disease dies out in the community. Also we established that when the basic reproduction number is greater than unity the disease persists. Utilizing optimal control theory, we explored the potential of time dependent education to eliminate the disease within 120 months. The model showed that time dependent education can be successful to minimize disease prevalence in the two patches, however, its success strongly depends on the total cost of implementation as well as its maximum strength.

1. Introduction

In the previous three decades the global community witnessed a major decline on the number of reported Guinea worm disease (GWD) cases, from 3.5 million in 20 countries in 1986 to only 22 cases in 2015 from only 4 countries, namely South Sudan, Mali, Chad and Ethiopia [3]. Prior studies have attributed this remarkable decline to the Guinea worm eradication program launched in the 1980s [3]. Despite this remarkable achievement, there are a couple of challenges that may thwart global eradication of the disease. Among many other challenges, continued use and sharing of open water sources by individuals from differential communities in GWD endemic countries remains a stumbling block to GWD eradication [3, 9, 24]. Individuals from different communities are known to have different behavior and knowledge about the disease [23]. Such heterogeneities have strong impacts on the dynamics of GWD, hence there is need to evaluate and quantify the possibility of GWD eradication under these circumstances.

GWD is a waterborne disease which infects humans when they drink unfiltered water containing copepods (small crustaceans) which are infected with larvae of *Dracunculus medinensis*. Once ingested, the copepods are destroyed by gastric

2010 *Mathematics Subject Classification.* 92D30, 49M05.
Key words and phrases. Mathematical model; Guinea worm disease; optimal control theory.

Submitted January 2, 2018. Published July 2, 2020.

juice in the human stomach, releasing the infective larvae [3, 7]. The released larvae will then migrate to small intestines where they penetrate through the duodenal wall and become adult worms in connective tissues. After maturation into adults and copulation, the male worm subsequently dies while the female worm grow into a full-size adult (length: 70 to 120 cm) [4]. After a year long incubation period, during which time the human host shows almost no symptoms, the female worm will migrate to other parts of the body, mostly on the distal lower extremity and induces a blister on the skin which ruptures leading to the emergence of the worm [6]. The itching and pain of the induced blister prompts the use of water as therapy, whereby infected individuals in rural communities often immerse their affected body part into water sources to get relief from the pain. Subsequently, the female worm releases thousands of its immature larvae (L1) [12]. These larvae are then ingested by copepods also called cyclops. Cyclops serve as intermediate host for *Dracunculus medinensis* [3]. Although GWD is rarely fatal, it may cause permanent disability and may result in loss of family income and school absenteeism [3, 13].

Since GWD has no vaccine or medicine the eradication programme has been based on the following preventive measures: provision of improved water sources, use of water filtration using different types of cloth or filament filters, health education to inform populations of how the infection is acquired and can be prevented, control of the intermediate host copepod using the larvicide, Abate, (temephos), containment of cases before they have an opportunity to contaminate water sources, active surveillance in endemic or previously endemic [24, 26].

In this paper, we aim to utilize a mathematical model to provide a comprehensive assessment on the impact of time dependent educational campaigns on controlling the spread of GWD in heterogeneous environment characterised by communities sharing a common open water source. Mathematical models play an important role in understanding and providing solutions to phenomena which are difficult to measure in the field [19, 22]. Only a few mathematical models have been contributed by researchers on the study of GWD (see, for example [1, 17, 18, 26, 31]). For example Adetunde, [1] investigated the current pattern of GWD in the northern region of Ghana. He analyzed the data from the region and proposed a time series model for the purpose of prediction. From his analysis it was observed that the number of infection cases reduces with time, implying that if the current trend continues then there is a likelihood that GWD will be completely eradicated. Recently, Link [17] proposed a compartment framework to study the dynamics of GWD. The author determined an algebraic solution to disease-free equilibrium and performed numerical stability analysis of the solution as well. Using the next generation matrix, Link determined the reproduction number $\mathbb{R}_0$ and found that the disease-free equilibrium is stable provided that the host visitation rate to the contaminated water sources is reduced. Smith? et al. [31] also developed a mathematical model for GWD. Impulsive differential equations were used to evaluate the effectiveness of chlorination. Latin Hypercube Sampling was used to determine model parameters that were highly sensitive to the basic reproduction number. From their work Smith? and co-workers established that education is the most effective intervention method, but a combination of education, chlorination and filtration will likely be required to achieve the final steps in the long journey to eradication.

Although these studies produced many useful results and improved the existing knowledge on GWD dynamics, however, none of these studies evaluated the

impact of time dependent educational campaigns on long term GWD dynamics in an environment where different communities share a common water source. This paper aims to fill this gap. The literature on epidemic models of the concurrent spread of infectious diseases and information is quite substantial (see, for example [5, 14, 25, 29, 30]). In [14], Joshi et al. used a deterministic compartmental model to demonstrate the effects of time dependent educational campaigns on lowering susceptibility classes and its impact on long term disease dynamics. Also, Samanta et al. [29], utilized a mathematical model to illustrate the effects of awareness programs by media on epidemic outbreaks. These studies, indeed, produced useful results and we will utilize some of the results to develop and analyze our framework.

The remainder of this paper is structured as follows. In Section 2, we present the methods and main results of the study. Precisely, we will analyze the dynamical behavior of the model, and perform an optimal control study for the implementation of educational campaigns. Analytical results in this section will be supported by numerical results constructed using MATLAB software. Section 3 provides a brief discussion to conclude the paper.

2. Mathematical model

We developed a mathematical model for GWD that comprises of two populations (patches) sharing a common water source. Although there are many possible network configurations here we considered a network of non-mixing patches with a single common water source, allowing patches to differ in the level of GWD awareness which in-turn affects their degree of risk to infection as well as their contribution to the pathogen population in the environment. This simple framework is motivated by living conditions in rural GWD endemic countries such as Ethiopia [3]. In rural Ethiopia, the provision of potable water supply remains a big challenge, for instance in one recent published study it was noted that only 42 out of 70 villages had access to safe drinking water [2]. Due to the unavailability of potable water supply, it was also noted that villagers in Ethiopia and other GWD endemic countries highly depend on water from open sources which are often shared by several communities [9]. According to Mari et al [23] different communities may be endowed with differential infection risk due to their geographical and/or socioeconomic factors. Heterogeneity in health education is one of the socio-economic factors that leads to differential in infection risk among individuals living within or in different communities.

To account for heterogeneity in this study we let the host population at time t in patch i by $N_i(t)$, $i = 1, 2$, such that $N(t) = N_1(t) + N_2(t)$. Further, we subdivided the total population of individuals in patch i into categories of: susceptible $S_i(t)$, exposed (latently infected) $E_i(t)$ and infectious $I_i(t)$, individuals. Meanwhile, let the dynamics of infected copepods in the environment be represented by compartment $W(t)$. Note that, here the intrinsic dynamics of the parasite have been neglected, as our aim is to provide a comprehensive, yet as simple as possible, account of the impact of heterogeneity in awareness on GWD dynamics. Therefore the proposed

model is governed by the following system of ordinary differential equations:

$$\begin{aligned}
\dot{S}_i(t) &= \Lambda_i - \beta_i(1-u_i)S_iW - \mu_i S_i,\\
\dot{E}_i(t) &= \beta_i(1-u_i)S_iW - (\alpha_i+\mu_i)E_i,\\
\dot{I}_i(t) &= \alpha_i E_i - (\kappa_i+\mu_i)I_i,\\
\dot{W}(t) &= (1-u_1)\gamma_1 I_1 + (1-u_2)\gamma_2 I_2 - \epsilon W.
\end{aligned} \tag{2.1}$$

All model variables and parameters are considered to be positive. Model parameter Λ_i denotes the constant recruitment rate of the host through birth and movement of susceptible individuals, μ_i is the natural mortality rate of the host; i.e., $\frac{1}{\mu_i}$ is the average life span, β_i account for indirect disease transmission rate, u_i represents the effects of health education on disease transmission, α_i is the incubation rate and it follows that $\frac{1}{\alpha_i}$ is the incubation period-for GWD and it ranges between 10–14 months [3], κ_i is the recovery rate; i.e., $\frac{1}{\kappa_i}$ is the average infectious period. Meanwhile, clinically infected individuals of patch i contribute to the parasite population in the environment at rate γ_i when they immerse their affected body part into water sources to get relief from the pain. Infected copepods die naturally at rate ϵ. Table 1 presents a summary of the model parameters and their baseline values.

TABLE 1. Description of model parameters and their baseline values

Var.	Definition	Value	Units	Source
β_1	Copepods ingestion rate for patch 1	1.2×10^{-5}	month^{-1}	[18]
β_2	Copepods ingestion rate for patch 2	$3\beta_1$	month^{-1}	
μ_i	Host natural death rate	0.0015	month^{-1}	[18]
ϵ	Parasite death rate	2.16	month^{-1}	[18]
α_i	Incubation rate	0.9996	month^{-1}	[18]
κ_i	Recovery rate	0.0083	month^{-1}	[18]
Λ_i	Host birth rate	100	Individ. month^{-1}	[18]
γ_1	Parasite shedding rate for patch 1	0.2	month^{-1}	[18]
γ_2	Parasite shedding rate for patch 2	0.2	month^{-1}	
u_i	Efficacy of educational campaigns in Path i	varied	Dimensionless	

Since model (2.1) represents human and pathogen population, all parameters in the model are non-negative and one can easily verify that all the solutions of the system are non-negative, given non-negative initial values. The model (2.1) will be analyzed in a biologically feasible region Ω defined as

$$\Big\{(N,W)\in\mathbb{R}^7_+ : N \le \frac{(\Lambda_1+\Lambda_2)}{[\min(\mu_1,\mu_2)]},\ W \le \frac{(\Lambda_1+\Lambda_2)((1-u_1)\gamma_1+(1-u_2)\gamma_2)}{[\epsilon\min(\mu_1,\mu_2)]}\Big\}.$$

Thus, the compact set Ω is positively invariant and attracting for model (2.1). Table 1 presents the model parameters and their baseline values.

Now, we compute the basic reproduction number of the model (2.1). The basic reproduction number $\mathbb{R}_0$, is arguably the most important quantity in infectious disease epidemiology. It can be utilized to account for the severity of the disease in the community whether epidemic or pandemic. To compute the basic reproduction

number of system (2.1) we need to determine the disease-free equilibrium (DFE) of the system. Thus, one can easily verify that system (2.1) has the following DFE

$$\mathcal{E}^0 = \big(S_1^0, S_2^0, E_1^0, E_2^0, I_1^0, I_2^0, W^0\big) = \Big(\frac{\Lambda_1}{\mu_1}, \frac{\Lambda_2}{\mu_2}, 0, 0, 0, 0, 0\Big).$$

Using the next-generation matrix notations in [32], the non-negative matrix F that denotes the generation of new infections and the non-singular matrix V that denotes the disease transfer among compartments, are respectively given by (at DFE)

$$F = \begin{bmatrix} 0 & 0 & 0 & 0 & \beta_1(1-u_1)S_1^0 \\ 0 & 0 & 0 & 0 & \beta_2(1-u_2)S_2^0 \\ 0 & 0 & 0 & 0 & 0 \\ 0 & 0 & 0 & 0 & 0 \end{bmatrix}, \quad V = \begin{bmatrix} m_1 & 0 & 0 & 0 & 0 \\ 0 & m_2 & 0 & 0 & 0 \\ -\alpha_1 & 0 & m_3 & 0 & 0 \\ 0 & -\alpha_2 & 0 & m_4 & 0 \\ 0 & 0 & -m_5 & -m_6 & \epsilon \end{bmatrix},$$

where

$$\begin{aligned} m_1 &= (\alpha_1 + \mu_1), \quad m_2 = (\alpha_2 + \mu_2), \\ m_3 &= (\kappa_1 + \mu_1), \quad m_4 = (\kappa_2 + \mu_2), \\ m_5 &= (1-u_1)\gamma_1, \quad m_6 = (1-u_2)\gamma_2. \end{aligned}$$

It follows that the spectral radius of system (2.1) is determined from $\rho(FV^{-1})$ and is given by

$$\mathbb{R}_0 = \frac{\beta_1\alpha_1(1-u_1)^2\gamma_1\Lambda_1}{\epsilon\mu_1 m_1 m_3} + \frac{\beta_2\alpha_2(1-u_2)^2\gamma_2\Lambda_2}{\epsilon\mu_2 m_2 m_4}. \tag{2.2}$$

The quantity $\mathbb{R}_0$ corresponds to the average number of secondary infections through environment-to-host transmission caused by one infectious individual in its infectious lifetime. Next, we investigate the existence of the endemic equilibrium point of model system (2.1).

Theorem 2.1. *Suppose $\mathbb{R}_0 > 1$. Then model system (2.1) admits a unique endemic equilibrium point.*

Proof. Let the endemic equilibrium of (2.1) be denoted by $\mathcal{E}^*(S_i^*, E_i^*, I_i^*, W^*)$, $i = 1, 2$. This steady state is determined by solving the system of equations

$$\begin{aligned} \Lambda_i - \beta_i(1-u_i)S_i^*W^* - \mu_i S_i^* &= 0, \\ \beta_i(1-u_i)S_i^*W^* - (\alpha_i + \mu_i)E_i^* &= 0, \\ \alpha_i E_i^* - (\kappa_i + \mu_i)I_i^* &= 0, \\ \sum_{i=1}^{2}(1-u_i)\gamma_i I_i^* - \epsilon W^* &= 0. \end{aligned} \tag{2.3}$$

For the third and fourth equations of (2.3) we have

$$E_i = \frac{(\kappa_i + \mu_i)}{\alpha_i} I_i^*, \quad W = \sum_{i=1}^{2} \frac{(1-u_i)\gamma_i}{\epsilon} I_i^*. \tag{2.4}$$

Substituting (2.4) into the second equation of (2.3) leads to

$$\sum_{i=1}^{2} \Big(\frac{\beta_i(1-u_i)\gamma_i S_i^*}{\epsilon} - \frac{(\kappa_i + \mu_i)(\alpha_i + \mu_i)}{\alpha_i}\Big) I_i^* = 0.$$

We can write

$$\sum_{i=1}^{2}\Big(\frac{\beta_i(1-u_i)^2\gamma_i\alpha_i S_i^*}{\epsilon(\kappa_i+\mu_i)(\alpha_i+\mu_i)}-1\Big)\frac{(\kappa_i+\mu_i)(\alpha_i+\mu_i)}{\alpha_i}I_i^*=0. \tag{2.5}$$

Equation (2.5) implies that

$$I_i^*=0,\quad \text{or}\quad S_i^*=\frac{\epsilon(\kappa_i+\mu_i)(\alpha_i+\mu_i)}{\beta_i(1-u_i)^2\gamma_i\alpha_i}=\frac{\Lambda_i}{\mu_i\mathbb{R}_i}.$$

From the first equation of (2.3) we have

$$\sum_{i=1}^{2}\Big(\Lambda_i-\beta_i(1-u_i)^2\frac{\Lambda_i}{\mu_i\mathbb{R}_i}\frac{\gamma_i}{\epsilon}I_i^*-\frac{\Lambda_i}{\mathbb{R}_i}\Big)=0,$$

and this gives

$$I_i^*=\frac{\epsilon\mu_i\mathbb{R}_i}{\beta_i(1-u_i)^2\gamma_i}\Big(1-\frac{1}{\mathbb{R}_i}\Big).$$

From (2.4) we have

$$E_i^*=\frac{\epsilon\mu_i(\kappa_i+\mu_i)\mathbb{R}_i}{\beta_i(1-u_i)^2\alpha_i\gamma_i}\Big(1-\frac{1}{\mathbb{R}_i}\Big),\quad W^*=\sum_{i=1}^{2}\frac{\mu_i\mathbb{R}_i}{\beta_i(1-u_i)^2}\Big(1-\frac{1}{\mathbb{R}_i}\Big).$$

As we can note, $\mathcal{E}^*$ exists whenever, $S_i^*>0$, $E_i^*>0$, $I_i^*>0$ and $W^*>0$ and this only feasible if $\mathbb{R}_0>1$. Therefore we conclude that the endemic equilibrium $\mathcal{E}^*$ exists and is unique whenever $\mathbb{R}_0>1$. □

Now, we are aware that model (2.1) has two unique equilibrium points and the existence of a unique endemic equilibrium implies that the disease will persist in the community if $\mathbb{R}_0>1$. Next, we carry out sensitivity analysis of $\mathbb{R}_0$ to infer the role of awareness campaigns on the average number of secondary cases that will be generated in the community. From the expression of the basic reproduction number (2.2) shows that changes in behavior of individuals from either patch due to awareness can lead to extinction or persistence of the disease, since

$$\lim_{(u_1\to 1,u_2\to 1)}\mathbb{R}_0=0,$$

and the reverse case leads to

$$\lim_{(u_1\to 0,u_2\to 0)}\mathbb{R}_0=\mathbb{R}_0^* \tag{2.6}$$

with

$$\mathbb{R}_0^*=\frac{\beta_1\alpha_1\gamma_1\Lambda_1}{\epsilon\mu_1 m_1 m_3}+\frac{\beta_2\alpha_2\gamma_2\Lambda_2}{\epsilon\mu_2 m_2 m_4},$$

note that $\mathbb{R}_0<\mathbb{R}_0^*$, for $u_i\neq 0$.

In what follows, we utilize numerical simulations to demonstrate the effects of different awareness levels on the basic reproduction number $\mathbb{R}_0$. As presented on Table 1, let patch 1 represent the less risk population while patch 2 represents the high risk population, such that disease transmission in the risk patch is three times that of low risk patch, that is, $\beta_2=3\beta_1$.

In Figure 1, a contour plot of the basic reproduction number $\mathbb{R}_0$ as a function of u_1 and u_2 is presented. Baseline values of other model parameters are based on Table 1. We can observe that there are many combinations of u_1 and u_2 that can lead to disease eradication, for instance if $u_1=0.4$, then the disease can be

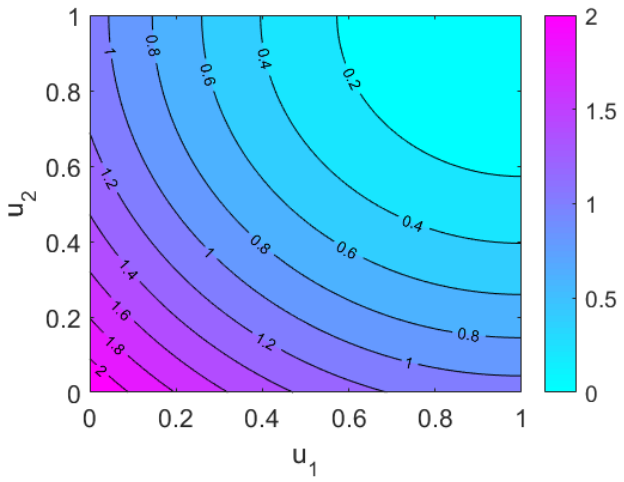

FIGURE 1. Contour plot illustrating the effects of different levels of awareness per patch on the basic reproduction number. Baseline values for parameters used are in Table 1

eliminated from the community if $u_2 \geq 0.3$, however, if $u_2 < 0.3$ then the infection will persist. Overall, we can conclude that if $u_i \geq 0.4$ in both patches then the infection will not persist in either of the patches.

In Figure 2 shows the effects of varying disease transmission rate and educational campaigns on the magnitude of the basic reproduction number. By varying u_i (with $u_1 = u_2$) and β_1, we observed that an increase in transmission rate in both patches will require an increase in educational campaigns for the disease to be eradicated, for instance when $\beta_1 = 4 \times 10^{-4}$ then educational campaigns equivalent to 0.7 or above will be needed to reduce the basic reproduction number to a value below unity.

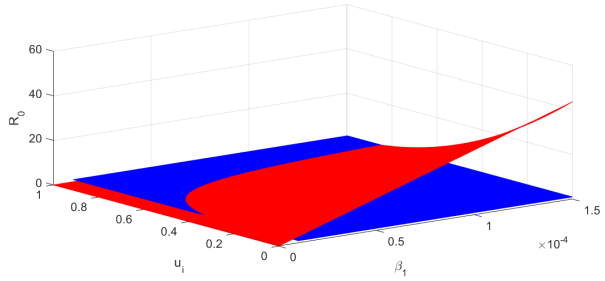

FIGURE 2. Effects of varying disease transmission rate and educational campaigns on the basic reproduction number. Parameter values used are in Table 1

Next, we determine the global stability of the disease-free equilibrium and the endemic equilibrium. The global stability of these equilibrium points will be investigated with the aid of Lyapunov functionals.

Theorem 2.2. *If $\mathbb{R}_0 \leq 1$, then the DFE is globally asymptotically stable in Ω.*

Proof. Consider the Lyapunov function

$$L(t) = \sum_{i=1}^{2} [a_i E_i(t) + b_i I_i(t)] + cW(t), \tag{2.7}$$

where

$$a_1 = \alpha_1\gamma_1 m_2 m_4, \quad a_2 = \alpha_2\gamma_2 m_1 m_3, \quad b_1 = \gamma_1 m_1 m_2 m_4,$$
$$b_2 = \gamma_2 m_1 m_2 m_3, \quad c = m_1 m_2 m_3 m_4.$$

Differentiating $L(t)$ along the solutions of the system (2.1) gives

$$\dot{L}(t) = \sum_{i=1}^{2} \big(a_i \dot{E}_i(t) + b_i \dot{I}_i(t)\big) + c\dot{W}(t).$$

Since $S_i \leq N_i \leq \Lambda_i/\mu_i$ for $i = 1, 2$, it follows that

$$\begin{aligned}
\dot{L}(t) &= \epsilon m_1 m_2 m_3 m_4 \Big(\sum_{i=1}^{2} \frac{\beta_i (1-u_i)^2 \alpha_i \gamma_i S_i}{\epsilon(\mu_i+\alpha_i)(\mu_i+\kappa_i)} - 1 \Big) W(t) \\
&\leq \epsilon m_1 m_2 m_3 m_4 \Big(\sum_{i=1}^{2} \frac{\beta_i (1-u_i)^2 \alpha_i \gamma_i \Lambda_i}{\epsilon\mu_i(\mu_i+\alpha_i)(\mu_i+\kappa_i)} - 1 \Big) W(t) \\
&= \epsilon m_1 m_2 m_3 m_4 \left(\mathbb{R}_0 - 1\right) W(t) \leq 0
\end{aligned}$$

provided that $\mathbb{R}_0 \leq 1$. When $\mathbb{R}_0 < 1$, $\dot{L} = 0$ yields $W = 0$. Then it can be easily observed from the system (2.1) that as $t \to \infty$, $E_i \to 0$, $I_i \to 0$, and $S_i \to S_i^0$, for $i = 1, 2$. Hence, the only invariant set when $\dot{L} = 0$ is the singleton $\mathcal{E}^0 = (S_1^0, S_2^0, 0, 0, 0, 0, 0)$. It follows from Lasalle's Invariance Principle [20] that every solution of the system (2.1), with initial conditions in Ω, approaches $\mathcal{E}^0$ as $t \to \infty$. Thus the equilibrium point $\mathcal{E}^0$ is globally asymptotically stable if $\mathbb{R}_0 < 1$. When $\mathbb{R}_0 = 1$, $\dot{L} = 0$ implies either $W = 0$, or

$$1 = \sum_{i=1}^{2} \frac{\beta_i (1-u_i)^2 \alpha_i \gamma_i S_i}{\epsilon(\mu_i+\alpha_i)(\mu_i+\kappa_i)} \leq \sum_{i=1}^{2} \frac{\beta_i (1-u_i)^2 \alpha_i \gamma_i \Lambda_i}{\epsilon\mu_i(\mu_i+\alpha_i)(\mu_i+\kappa_i)} = \mathbb{R}_0 = 1.$$

The latter case yields $S_i = S_i^0$ and, consequently, $E_i = I_i = W = 0$ for $i = 1, 2$. Hence, in either case, the only invariant set for $\dot{L} = 0$ is the singleton $\mathcal{E}^0 = (S_1^0, S_2^0, 0, 0, 0, 0, 0)$. Therefore the equilibrium point $\mathcal{E}^0$ is globally asymptotically stable if $\mathbb{R}_0 = 1$. □

In contrast, if $\mathbb{R}_0 > 1$, then by continuity, $\dot{L}(t) > 0$ in a neighbourhood of $\mathcal{E}^0$ in $\hat{\Omega}$. Solutions in $\hat{\Omega}$ sufficiently close to $\mathcal{E}^0$ move away from $\mathcal{E}^0$ implying that the DFE is unstable. Applying a uniform persistence result from [11] and an argument as in the proof of [16, Prop. 3.3], it can be shown that, if $\mathbb{R}_0 > 1$, instability of $\mathcal{E}^0$ implies uniform persistence of the system (2.1).

Next, we study the global stability of the positive endemic equilibrium $\mathcal{E}^*$. The problem is generally difficult for systems with dimensions higher than two. Following the approach used in [8], we introduce the following assumptions for our model (2.1):

(A1) There exist a family of functions $\Phi_i(S_i) : (0, \frac{\Lambda_i}{\mu_i}] \to \mathbb{R}_+$, $i = 1, 2$, Such that for all S_i, E_i, $W > 0$,

$$[S_i - S_i^*]\,[\Phi_i(S_i) - \Phi_i(S_i^*)] \geq 0,$$
$$\Big[\frac{f_i(S_i, W)\Phi_i(S_i^*)}{f_i(S_i^*, W^*)\Phi_i(S_i)} - 1\Big]\Big[1 - \frac{f_i(S_i^*, W^*)\Phi_i(S_i)E_i}{f_i(S_i, W)\Phi_i(S_i^*)E_i^*}\Big] \leq 0.$$

(A2) For all E_i, $I_i > 0$, $1 \leq i \leq 2$,

$$\big[\frac{E_i}{E_i^*} - 1\big]\big[1 - \frac{E_i^* I_i}{E_i I_i^*}\big] \leq 0. \tag{2.8}$$

(A3) For all I_i, $W > 0$, $1 \leq i \leq 2$,

$$\big[\frac{g_i(I_i)}{g_i(I_i^*)} - 1\big]\big[1 - \frac{g_i(I_i^*)W}{g_i(I_i)W^*}\big] \leq 0.$$

These assumptions are motivated by the proof of [8, Theorem 6.1]. The functions Φ_i, for example, can be taken as $\Phi_i(S_i) = S_i$ for $i = 1, 2$. We now prove that if $\mathbb{R}_0 > 1$ then the endemic equilibrium point is globally asymptotically stable.

Theorem 2.3. *If $\mathbb{R}_0 > 1$ then the endemic equilibrium point of system $\mathcal{E}^*$ exists and is globally asymptotically stable.*

Proof. Consider the Lyapunov function

$$\mathcal{V}(t) = \sum_{i=1}^{2} \Big\{ \int_{S_i^*}^{S_i} \frac{\Phi_i(\xi) - \Phi_i(S_i^*)}{\Phi_i(\xi)} d\xi + \big[E_i - E_i^* - E_i^* \ln \frac{E_i}{E_i^*}\big] + \big[I_i - I_i^* - I_i^* \ln \frac{I_i}{I_i^*}\big]\Big\} + \big[W - W^* - W^* \ln \frac{W}{W^*}\big].$$

At endemic equilibrium we have the following identities

$$\begin{aligned} \Lambda_i &= f_i(S_i^*, W^*) + \mu_i S_i^*, \\ (\alpha_i + \mu_i)E_i^* &= f_i(S_i^*, W^*), \\ (\kappa_i + \mu_i)I_i^* &= \alpha_i E_i^*, \\ \epsilon W^* &= \sum_{i=1}^{2} g(I_i^*). \end{aligned} \tag{2.9}$$

Differentiating $\mathcal{V}$ along the solutions of (2.1) and using the equilibrium equations (2.9), we obtain

$$\begin{aligned} \frac{d\mathcal{V}}{dt} &= \sum_{i=1}^{2} \Big\{ \big[1 - \frac{\Phi_i(S_i^*)}{\Phi_i(S_i)}\big]\frac{dS_i}{dt} + \big[1 - \frac{E_i^*}{E_i}\big]\frac{dE_i}{dt} + \big[1 - \frac{I_i^*}{I_i}\big]\frac{dI_i}{dt}\Big\} \\ &\quad + \big[1 - \frac{W^*}{W}\big]\frac{dW}{dt} \\ &= \sum_{i=1}^{2} \Big\{ \big[1 - \frac{\Phi_i(S_i^*)}{\Phi_i(S_i)}\big][f_i(S_i^*, W^*) + \mu_i S_i^* - f_i(S_i, W) - \mu_i S_i] \\ &\quad + \big[f_i(S_i, W) - f_i(S_i, W)\frac{E_i^*}{E_i} - f_i(S_i^*, W^*)\frac{E_i}{E_i^*} + f_i(S_i^*, W^*)\big] \\ &\quad + \Big[\alpha_i E_i - \alpha_i E_i \frac{I_i^*}{I_i} - \alpha_i E_i^* \frac{I_i}{I_i^*} + \alpha_i E_i^*\Big] \end{aligned}$$

$$+\Big[g_i(I_i)-g_i(I_i)\frac{W^*}{W}-g_i(I_i^*)\frac{W}{W^*}+g_i(I_i^*)\Big]\Big\}.$$

After some algebraic manipulations, we have

$$\begin{aligned}\frac{d\mathcal{V}}{dt}&=\sum_{i=1}^{2}\Big\{\frac{-\mu_i}{\Phi_i(S_i)}[S_i-S_i^*][\Phi_i(S_i)-\Phi_i(S_i^*)]\\&\quad+f_i(S_i^*,W^*)\Big[\frac{f_i(S_i,W)\Phi_i(S_i^*)}{f_i(S_i^*,W^*)\Phi_i(S_i)}-1\Big]\Big[1-\frac{f_i(S_i^*,W^*)\Phi_i(S_i)E_i}{f_i(S_i,W)\Phi_i(S_i^*)E_i^*}\Big]\\&\quad+f_i(S_i^*,W^*)\Big[3-\frac{\Phi_i(S_i^*)}{\Phi_i(S_i)}-\frac{f_i(S_i,W)E_i^*}{f_i(S_i^*,W^*)E_i}-\frac{f_i(S_i^*,W^*)\Phi_i(S_i)E_i}{f_i(S_i,W)\Phi_i(S_i^*)E_i^*}\Big]\\&\quad+\alpha_iE_i^*\Big[\frac{E_i}{E_i^*}-1\Big]\Big[1-\frac{E_i^*I_i}{E_iI_i^*}\Big]+\alpha_iE_i^*\Big[2-\frac{E_iI_i^*}{E_i^*I_i}-\frac{E_i^*I_i}{E_iI_i^*}\Big]\\&\quad+g_i(I_i^*)\Big[\frac{g_i(I_i)}{g_i(I_i^*)}-1\Big]\Big[1-\frac{g_i(I_i^*)W}{g_i(I_i)W^*}\Big]\\&\quad+g_i(I_i^*)\Big[2-\frac{g_i(I_i)W^*}{g_i(I_i^*)W}-\frac{g_i(I_i^*)W}{g_i(I_i)W^*}\Big]\Big\}.\end{aligned}$$

It follows from assumptions (A1)–(A3) that

$$\begin{aligned}\frac{d\mathcal{V}}{dt}&\le\sum_{i=1}^{2}\Big\{f_i(S_i^*,W^*)\Big[3-\frac{\Phi_i(S_i^*)}{\Phi_i(S_i)}-\frac{f_i(S_i,W)E_i^*}{f_i(S_i^*,W^*)E_i}-\frac{f_i(S_i^*,W^*)\Phi_i(S_i)E_i}{f_i(S_i,W)\Phi_i(S_i^*)E_i^*}\Big]\\&\quad+\alpha_iE_i^*\Big[2-\frac{E_iI_i^*}{E_i^*I_i}-\frac{E_i^*I_i}{E_iI_i^*}\Big]+g_i(I_i^*)\Big[2-\frac{g_i(I_i)W^*}{g_i(I_i^*)W}-\frac{g_i(I_i^*)W}{g_i(I_i)W^*}\Big]\Big\}\\&\le 0.\end{aligned}$$

The terms inside the square brackets are non-positive due to the fact that the geometric mean is less than or equal to the arithmetic mean:

$$\begin{aligned}&\frac{\Phi_i(S_i^*)}{\Phi_i(S_i)}+\frac{f_i(S_i,W)E_i^*}{f_i(S_i^*,W^*)E_i}+\frac{f_i(S_i^*,W^*)\Phi_i(S_i)E_i}{f_i(S_i,W)\Phi_i(S_i^*)E_i^*}\\&\ge 3\sqrt[3]{\frac{\Phi_i(S_i^*)}{\Phi_i(S_i)}.\frac{f_i(S_i,W)E_i^*}{f_i(S_i^*,W^*)E_i}.\frac{f_i(S_i^*,W^*)\Phi_i(S_i)E_i}{f_i(S_i,W)\Phi_i(S_i^*)E_i^*}}=3,\\&\frac{E_iI_i^*}{E_i^*I_i}+\frac{E_i^*I_i}{E_iI_i^*}\ge 2\sqrt{\frac{E_iI_i^*}{E_i^*I_i}\cdot\frac{E_i^*I_i}{E_iI_i^*}}=2,\\&\frac{g_i(I_i)W^*}{g_i(I_i^*)W}+\frac{g_i(I_i^*)W}{g_i(I_i)W^*}\ge 2\sqrt{\frac{g_i(I_i)W^*}{g_i(I_i^*)W}.\frac{g_i(I_i^*)W}{g_i(I_i)W^*}}=2.\end{aligned}$$

Meanwhile, it can be easily observed that the largest invariant set where $\dot{\mathcal{V}}=0$ is the singleton $\{\mathcal{E}^*\}$. Hence, by LaSalle's invariance principle, $\mathcal{E}^*$ is globally asymptotically stable. This completes the proof of Theorem. □

In Figure 3 phase portraits were constructed to illustrate the convergence of solutions to the disease-free and endemic equilibrium for $\mathbb{R}_0<1$ and $\mathbb{R}_0>1$, respectively. In Figure 3 (a) one can observe that all the three solution orbits converge to the disease-free equilibrium over time whenever $\mathbb{R}_0<1$ as guaranteed by Theorem 2.2. However, whenever $\mathbb{R}_0>1$ we can also note that the solution orbits converge to the endemic point, as illustrated in Figure 3 (b).

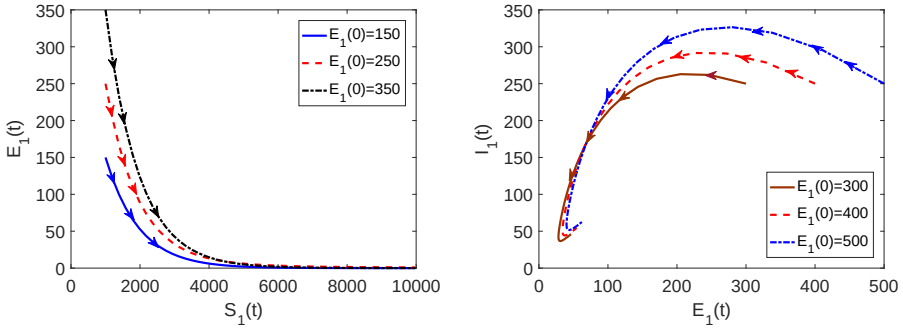

(a) (b)

FIGURE 3. Phase portraits illustrating the converge of solutions to the (a) disease-free equilibrium when $\mathbb{R}_0 < 1$, (b) endemic equilibrium when $\mathbb{R}_0 > 1$. To construct the phase portrait in (a) we set $u_1 = 0.55$ and $u_2 = 0.45$ to obtain $\mathbb{R}_0 = 0.983$ and for (b) we set $u_1 = 0.3$ and $u_2 = 0.1$ to obtain $\mathbb{R}_0 = 2.56$. In addition, the initial population levels were set to $S(0)_i = 1000$, $E_2(0) = 0$, $I_1 = I_2 = 0$ and $W(0) = 500$. In (a) we can observe that all the three solution orbits converge to the disease-free equilibrium demonstrating that whenever $\mathbb{R}_0 < 1$ the disease dies out in the community as guaranteed by Theorem 2.2. However, if $\mathbb{R}_0 > 1$ we can see that the disease persists since the solution orbits converge to the endemic point.

3. Formulation and analysis of the optimal control problem

In this section, we apply optimal control theory to identify optimal educational campaign strategies for GWD management. Thus the constant educational campaigns parameter u_i considered earlier in model (2.1), is now assumed to be time dependent, i.e. $u_i(t)$ $i = 1, 2$. Utilizing the same variables and parameters names as before, our model with time dependent controls is given by

$$\begin{aligned}
\dot{S}_i(t) &= \Lambda_i - \beta_i(1 - u_i(t))S_i(t)W(t) - \mu_i S_i(t),\\
\dot{E}_i(t) &= \beta_i(1 - u_i(t))S_i(t)W(t) - (\alpha_i + \mu_i)E_i(t),\\
\dot{I}_i(t) &= \alpha_i E_i(t) - (\kappa_i + \mu_i)I_i(t),\\
\dot{W}(t) &= \gamma(1 - u_1(t))I_1 + \gamma(1 - u_2(t))I_2 - \epsilon W.
\end{aligned} \tag{3.1}$$

Our goal is to minimize the numbers of clinically infected individuals over a finite time horizon $[0, T]$ at minimal costs in each patch. Mathematically, we formulate an objective functional $J(u(t))$ as follows:

$$J\big(u_1(t), u_2(t)\big) = \int_0^T \Big(A_1 I_1(t) + \frac{B_1}{2}u_1^2(t) + A_2 I_2(t) + \frac{B_2}{2}u_2^2(t)\Big)\, dt\,, \tag{3.2}$$

where A_i and B_i, $i = 1, 2$, are balancing coefficients (positive) transferring the integral into monetary quantity over a finite period of time. Note that the control efforts are assumed to be nonlinear, due to a number of advantages associated with a nonlinear function on the control. One of the advantages is that a nonlinear

control allows the Hamiltonian to attain its minimum over the control set at a unique point. Moreover, a quadratic structure in the control has mathematical advantages. We seek an optimal control pair $(u_1^*, u_2^*) \in U$ such that

$$J(u_1^*, u_2^*) = \inf_{(u_1,u_2)\in U} J(u_1, u_2) \tag{3.3}$$

for the admissible set $U = \{(u_1, u_2) \in (L^\infty(0,T))^2 : 0 \le u_i \le a_i; a_i \in \mathbb{R}^+, i = 1, 2\}$. The following theorem states the existence of the solution of the system (3.1) as well as their non-negativity and boundedness.

Theorem 3.1. *Given $u = (u_1, u_2) \in U$, there exists a non-negative bounded solution (S_i, E_i, I_i, W) $i = 1, 2$ to the state system* (3.1) *on the finite interval $[0, T]$ with given initial conditions.*

Proof. Since the controls and the state variables are uniformly bounded and non-negative on the finite interval $[0, T]$, there exists a minimizing sequence (u_1^n, u_2^n) such that

$$\lim_{n\to\infty} J(u_1^n, u_2^n) = \inf_{(u_1,u_2)\in U} J(u_1, u_2).$$

We denote the corresponding sequence of the state variables by (S_i, E_i, I_i, W_i) $i = 1, 2$. Further, since all state and control variables are bounded, then derivatives of the state variables are also bounded and it follows that all state variables are Lipschitz continuous with the same Lipschitz constant. Thus the sequence (S_i, E_i, I_i, W_i) $i = 1, 2$ is uniformly equicontinuous in $[0, T]$. Therefore by the Arzela-Ascoli Theorem [21, 27], the state sequence has a subsequence that converges uniformly to $(S_i^*, E_i^*, I_i^*, W_i^*)$ $i = 1, 2$ in $0, T]$. Hence the control sequence $u_n^n = (u_1^n, u_2^n)$ has a subsequence that converges weakly in $L^2(0, T)$. Let $(u_1^*, u_2^*) \in U$ be such that $u_i^n \rightharpoonup u_i^*$ weakly in $L^2(0, T)$ for $i = 1, 2$. utilizing the lower semi-continuity norms in weak L^2, we obtain

$$\|u_i^*\|_{L^2}^2 \le \lim_{n\to\infty} \|u_i^n\|_{L^2}^2, \quad for i = 1, 2. \tag{3.4}$$

Hence,

$$\begin{aligned} J(u_1^*, u_2^*) &\le \lim_{n\to\infty} \int_0^T \big[A_1 I_1^n(t) + \frac{B_1}{2} u_1^n(t) + A_2 I_2^n(t) + \frac{B_2}{2} u_2^n(t)\big] dt \\ &= \lim_{n\to\infty} J(u_1, u_2). \end{aligned}$$

Thus, we conclude that there exists a pair of control (u_1^*, u_2^*) that minimizes the objective functional $J(u_1, u_2)$. □

By utilizing the result from Lukes [21] one can easily verify the existence and uniqueness of solutions for the state system (3.1) with a given control pair. Since there exists an optimal control from Theorem 3.1, now we can apply Pontryagin's Maximum Principle [28]. Thus, the optimal control system (3.1) is converted into an equivalent problem of minimizing the Hamiltonian

$$\begin{aligned} H(t) = A_1 I_1(t) + A_2 I_2(t) &+ \frac{B_1}{2} u_1^2(t) + \frac{B_2}{2} u_2^2(t) \\ &+ \lambda_{S_1}\Big\{\Lambda_1 - [1 - u_1(t)]\beta_1 S_1 W - \mu_1 S_1\Big\} \\ &+ \lambda_{S_2}\Big\{\Lambda_2 - [1 - u_2(t)]\beta_2 S_2 W - \mu_2 S_2\Big\} \end{aligned}$$

$$
\begin{aligned}
&+ \lambda_{E_1}\Big\{[1-u_1(t)]\beta_1 S_1 W - (\alpha_1+\mu_1)E_1\Big\}\\
&+ \lambda_{E_2}\Big\{(1-u_2(t))\beta_2 S_2 W - (\alpha_2+\mu_2)E_2\Big\}\\
&+ \lambda_{I_1}\Big\{\alpha_1 E_1 - (\kappa_1+\mu_1)I_1\Big\} + \lambda_{I_2}\Big\{\alpha_2 E_2 - (\kappa_2+\mu_2)I_2\Big\}\\
&+ \lambda_W\Big\{(1-u_1(t))\gamma_1 I_1 + (1-u_2(t))\gamma_2 I_2 - \epsilon W\Big\},
\end{aligned}
$$

where $\lambda_{S_i}(t)$, $\lambda_{E_i}(t)$, $\lambda_{I_i}(t)$ $(i=1,2)$ and $\lambda_W(t)$ denote the adjoint functions associated with the states S_i, E_i, I_i and W, $i=1,2$ respectively. Note that, in H, each adjoint function multiplies the right-hand side of the differential equation of its corresponding state function. The first term in H comes from the integrand of the objective functional.

Given an optimal control pair $u=(u_1,u_2)\in U$ and corresponding states (S_i,E_i,I_i,W), $i=1,2$ there exist adjoint functions [15] satisfying

$$
\frac{d\lambda_{S_i}(t)}{dt} = -\frac{\partial H}{\partial S_i}, \quad \frac{d\lambda_{E_i}(t)}{dt} = -\frac{\partial H}{\partial E_i}, \quad \frac{d\lambda_{I_i}(t)}{dt} = -\frac{\partial H}{\partial I_i}, \quad \frac{d\lambda_W(t)}{dt} = -\frac{\partial H}{\partial W}.
$$

These equalities give

$$
\begin{aligned}
\dot\lambda_{S_1}(t) &= \mu_1\lambda_{S_1}(t) + \beta_1[1-u_1(t)][\lambda_{S_1}(t)-\lambda_{E_1}(t)]W(t),\\
\dot\lambda_{S_2}(t) &= \mu_2\lambda_{S_2}(t) + \beta_2[1-u_2(t)][\lambda_{S_2}(t)-\lambda_{E_2}(t)]W(t),\\
\dot\lambda_{E_1}(t) &= \mu_1\lambda_{E_1}(t) + \alpha_1[\lambda_{E_1}(t)-\lambda_{I_1}(t)],\\
\dot\lambda_{E_2}(t) &= \mu_2\lambda_{E_2}(t) + \alpha_2[\lambda_{E_2}(t)-\lambda_{I_2}(t)],\\
\dot\lambda_{I_1}(t) &= -A_1 + (\kappa_1+\mu_1)\lambda_{I_1}(t) - (1-u_1)\gamma_1\lambda_W(t),\\
\dot\lambda_{I_2}(t) &= -A_2 + (\kappa_2+\mu_2)\lambda_{I_2}(t) - (1-u_2)\gamma_2\lambda_W(t),\\
\dot\lambda_W(t) &= \epsilon\lambda_W(t) + \beta_1[1-u_1(t)][\lambda_{S_1}(t)-\lambda_{E_1}(t)]S_1(t)\\
&\quad + \beta_2[1-u_2(t)][\lambda_{S_2}(t)-\lambda_{E_2}(t)]S_2(t),
\end{aligned}
\tag{3.5}
$$

with transversality conditions $\lambda_j(T)=0$ for $j=S_i(t)$, $E_i(t)$, $I_i(t)$ $(i=1,2)$ and $W(t)$. Furthermore, the optimal controls are characterized by the optimality condition:

$$
\begin{aligned}
u_1(t) &= \min\Big(\max\Big(0,\frac{\beta_1 S_1 W(\lambda_{E_1}-\lambda_{S_1})+\gamma_1 I_1\lambda_W}{B_1}\Big), a_1\Big),\\
u_2 &= \min\Big(\max\Big(0,\frac{\beta_2 S_2 W(\lambda_{E_2}-\lambda_{S_2})+\gamma_2 I_2\lambda_W}{B_2}\Big), a_2\Big).
\end{aligned}
\tag{3.6}
$$

Finally, for sufficiently large T, one can show the uniqueness of an optimal control pair by following the approach in [10]. Our optimal control problem thus couples the state system (3.1), the adjoint system (3.5), and the optimality condition (3.6). These equations are solved numerically using the forward-backward sweeping method [15], based on parameters listed in Table 1 and the following assumed initial population levels:

$$
S_i(0)=1000, \quad E_i(0)=50, \quad I_i(0)=100, \quad W(0)=500, \quad i=1,2.
$$

In particular, we will find the simulation results under two different cases: Case A: Homogeneous setting, that is, disease characteristics are the same in the two patches. Case B: Heterogeneous setting, that is, different disease characteristics

between the two patches. For each case, we find the total number of new infections in the two patches by the formula

$$T_n = \int_0^T \Big(\beta_1(1-u_1)S_1 + \beta_2(1-u_2)S_2\Big)W\,dt. \tag{3.7}$$

Recall that the total cost associated with infected humans and the controls J, is given by equation (3.2).

Case A: Homogeneous setting. To account for homogeneous setting, we assume equal disease transmission rate and educational campaigns, that is, we set $\beta_1 = \beta_2 = 3.6 \times 10^{-5}$, and $0 \le u_i(t) \le 0.6$. We set the initial guess of the controls as follows $u_1 = u_2 = 0.3$ and these values also correspond to educational campaign levels in the absence of time dependent intervention strategies. Furthermore, we set the weight constant to $A_1 = A_2 = 1$, $B_1 = B_2 = 10$, and the numerical illustrations are presented in Figure 4.

From Figure 4, we observe that when disease characteristics (initial population levels and model parameters) are the same in the two patches then the dynamics of the disease will be similar in both patches. However, in the absence of optimal control we can see that the total number of exposed and infectious individuals will be higher compared to when there is optimal control. In particular, with optimal control implemented, the infected host population for both patches reduces remarkably to levels close to zero. Precisely, over a period of 120 months, the total number of new infections that will be generated from the two patches in the absence of optimal control is 1.2037×10^4, whereas, with optimal control approximately 408 infections and the total cost is $J = 990$. These results suggests that the presence of optimal control may lead to a reduction of approximately 1.1629×10^4 infections over a period of 120 months. Figure 4 (d) shows the optimal control profile for $u_i(t)$, $i = 1, 2$. As we can observe the control profile for u_i starts from its maximum $u_i = 0.6$ and remains there till the final time horizon, where it will drop to the origin. Thus, for effective GWD management time dependent educational campaigns will have to be maintained at maximum intensity for the entire horizon suggesting that perhaps, educational campaigns may need to be combined with other less cost intervention strategies (such as filtering water using pieces of cloth) in order to minimize cumulative costs in the long run.

TABLE 2. Total number of newly infected humans over 120 months and the total cost J with respect to control bounds, under the homogeneous scenario. The balancing constants were set to $A_i = 1$ and $B_i = 10$, for $i = 1, 2$.

Upper bounds of a_i	Total cost J	Number of new infections T_n
0.4	2.0256×10^4	1.8389×10^4
0.6	990.0536	408
0.8	915.1205	52

From Table 2, we can observe that as the upper bound of u_i approaches 1, the total number of newly infected individuals and total cost decreases significantly.

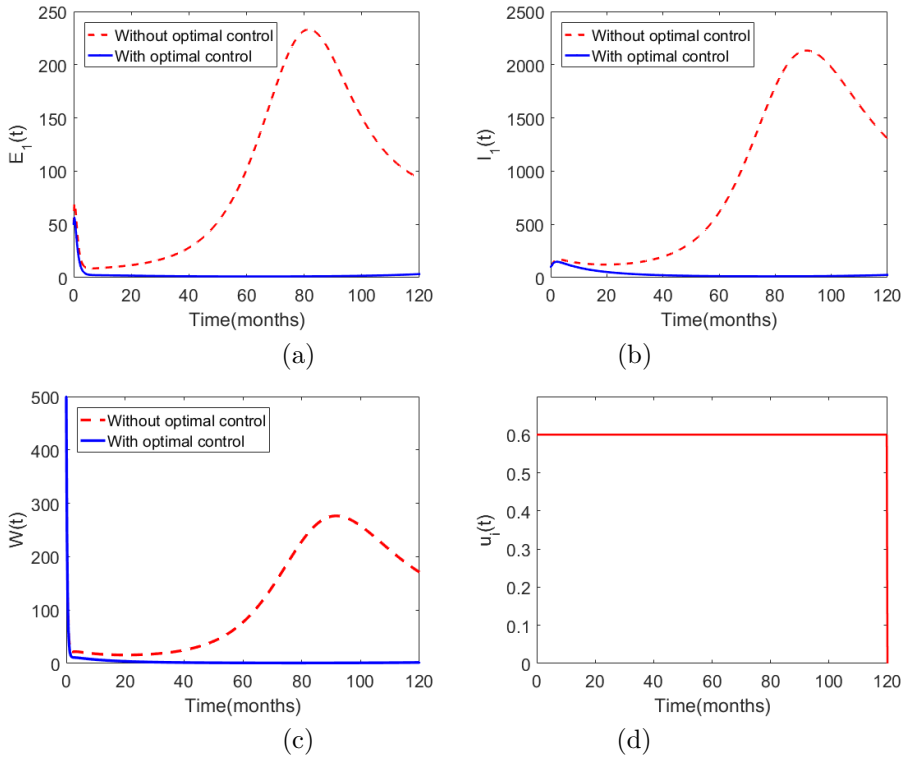

FIGURE 4. Simulation results for case A: homogeneous setting. The solid curves in (a)-(c) represent the population levels of the host and vector in the presence of optimal control while the dotted lines depict the population levels in the absence of optimal control. The time varying educational rate is plotted in (d), $0 \leq u_i(t) \leq 0.6$. Note that since equality is assumed for both patches the diseases dynamics are similar, thus $E_1(t) = E_2(t)$, $I_1(t) = I_2(t)$, $u_1(t) = u_2(t)$.

Case B: Heterogeneous setting. Although case A (Homogeneous setting), is highly impractical it serves to demonstrate the likely outcome under homogeneous conditions and allows comparison to be made with the real world scenario – the heterogeneous setting. Here, we will investigate the impact of heterogeneous diseases characteristics between the two patches on long term disease dynamics. In particular we will investigate heterogeneity on (i) disease transmission rates, with the assumption that $\beta_2 = 6\beta_1$ (ii) bounds of the controls $a_2 < a_1$ (iii) both disease transmission rates and upper bounds of the controls. For all the simulations in case B we set the initial guess for the control as $u_1 = 0.4$,and $u_2 = 0.3$ and these values also correspond to education campaign levels in the absence of optimal control.

Figure 5 depicts the time evolution of the infected host and pathogen in patches 1 and 2, for the scenario with and without the optimal control, under heterogeneous disease transmission rates ($\beta_2 = 6\beta_1$, with $\beta_1 = 3.6 \times 10^{-4}$) and similar bounds of the controls ($0 \leq u_i(t) \leq 0.8$). As we have already observed, the presence of

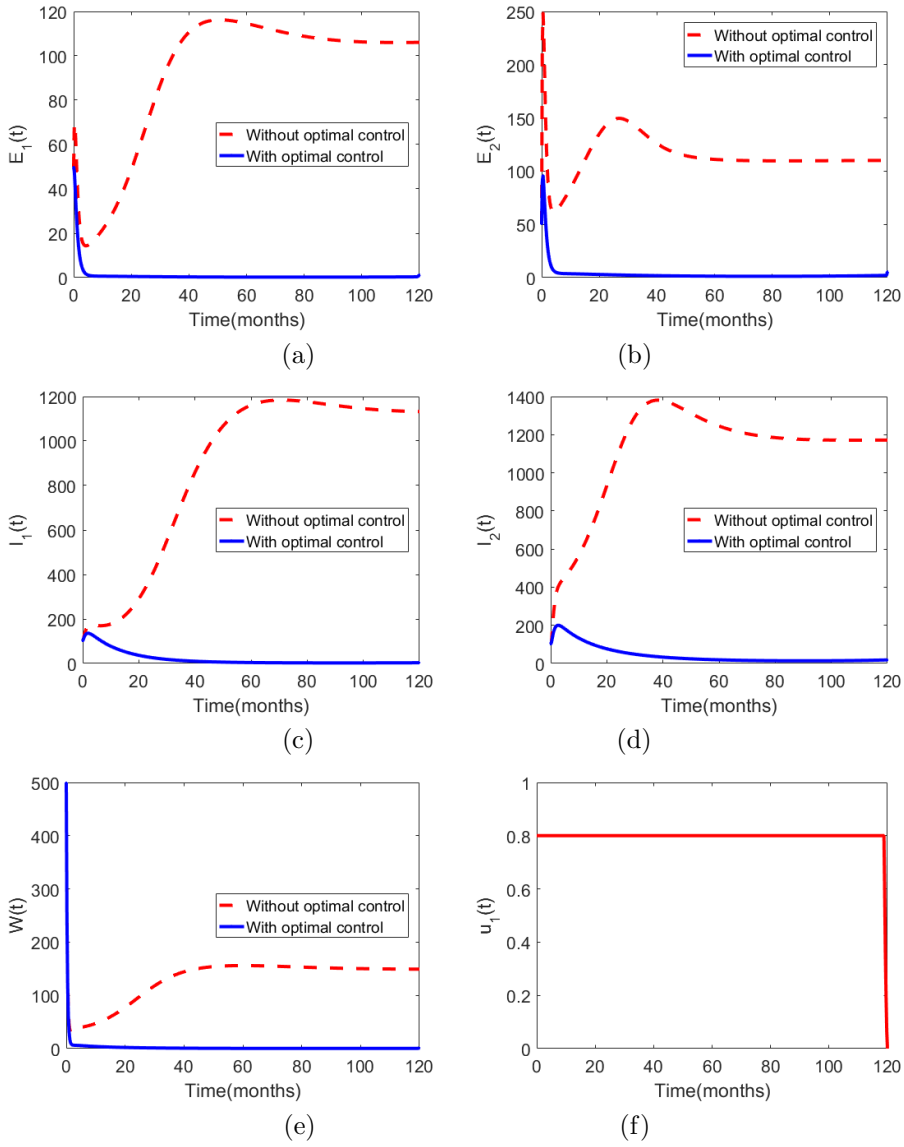

FIGURE 5. Solution of the model (asymptomatic individuals) with and without optimal control under heterogeneous setting, with $0 \leq u_i(t) \leq 0.8$. The control profile for $u_2(t)$ has been omitted since it has exactly the same pattern as $u_1(t)$

optimal control will be associated with extremely low new infections as compared to when they is no optimal control. Precisely, in the absence of optimal control approximately a total of 3.535×10^3 new infections will generated compared to approximately 98, over a period of 120 months. The total cost of implementing the strategy will be $J = 1.258 \times 10^3$.

TABLE 3. Total number of newly infected humans over 120 months and the total cost J with respect to control bounds, under the heterogeneous disease transmission between the two patches. The balancing constants were set to $A_i = 1$ and $B_i = 10$, $0 \le u_i(t) \le 0.8$ for $i = 1, 2$, with $\beta_1 = 3.6 \times 10^{-4}$.

Transmission rate β_2	Total cost J	Number of new infections T_n
$3\beta_1$	1.010×10^3	62
$6\beta_1$	1.258×10^3	98
$9\beta_1$	2.193×10^3	256
$12\beta_1$	5.735×10^3	784

Table 3 depicts the effects of heterogeneous disease transmission rates between the two patches. As we can observe, an increase in disease transmission rate for the risk patch (patch 2) will lead to an increase on the total number of new infections and total cost over a period of 120 months. For instance, an increase on disease transmission rate from $6\beta_1$ to $9\beta_1$ will increase the total number of new infections by more than 100%. Furthermore, we can also observe that increasing disease transmission rate in patch 2 from $9\beta_1$ to $12\beta_1$ will also be associated with more than 100% increase on the total number of new infections and total costs over the same period.

Numerical illustrations in Figure 6 illustrates the impact of different upper bound to controls u_1 and u_2 (that is, $0 \le u_1 \le 0.8$ and $0 \le u_2 \le 0.5$). As once observed earlier, the total number of new infections will be high in the absence of optimal control compared to when there is optimal control. In particular, approximately a total of 1.086×10^4 infections will be generated when there is no time dependent intervention strategies compared to approximately 260 in the presence of time dependent controls, over the same period of 120 months. The total cost associated with strategy implementation is $J = 927.86$. Figure 6 (d) shows the control profiles for controls u_1 and u_2, and we can observe that all the control profiles starts at their maximum till the final time horizon where they will drop sharply to the origin. This suggests that for effective disease management educational campaigns will have to be maintained at their maximum intensities in both patches over 120 months.

Simulations in Figure 7 demonstrates the effects of heterogeneous on: disease transmission rates, upper bound of the controls and initial population levels between the two patches, on long term disease dynamics. In particular, we have assumed higher disease transmission rate, lower upper bound to the control and higher initial population levels for patch 2-assumed to be the high risk community compared to patch 1. Under these circumstances we observed that approximately 8.51×10^3 new infections will be generated in the absence of optimal control compared to approximately 1.673×10^3 infections in the presence of optimal control over a period of 120 months. In addition, the total cost of implementing the time dependent strategies is $J = 3.254 \times 10^3$.

Table 4 presents a summary of the variations in the weight parameters and their corresponding effects, under a heterogeneous scenario. Overall, we can observe that as these various weight constants increase the total cost J and the total number of new infections increases significantly. In particular, an increase in B_i leads

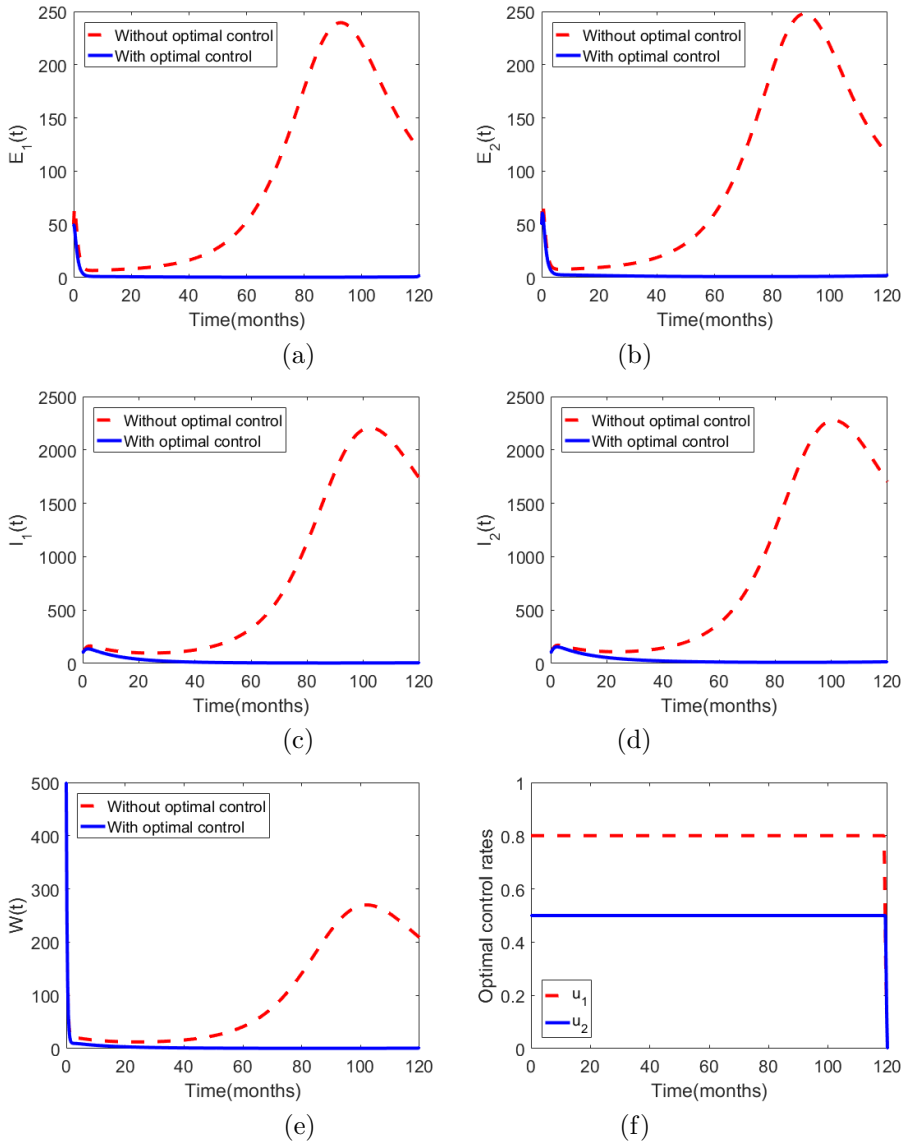

FIGURE 6. Simulation results for case B, illustrating the dynamics of exposed individuals, infectious individuals and the pathogen in the environment, with and without optimal control, for $0 \leq u_1 \leq 0.8$, $0 \leq u_2 \leq 0.5$, $\beta_1 = \beta_2 = 3.6 \times 10^{-4}$. The solid curves in (a)-(e) represent the population levels of the host and pathogen in the presence of optimal control while the dotted lines depict the population levels without optimal control.

to remarkable changes on the total cost and the total number of new infections compared to A_i, for $i = 1, 2$.

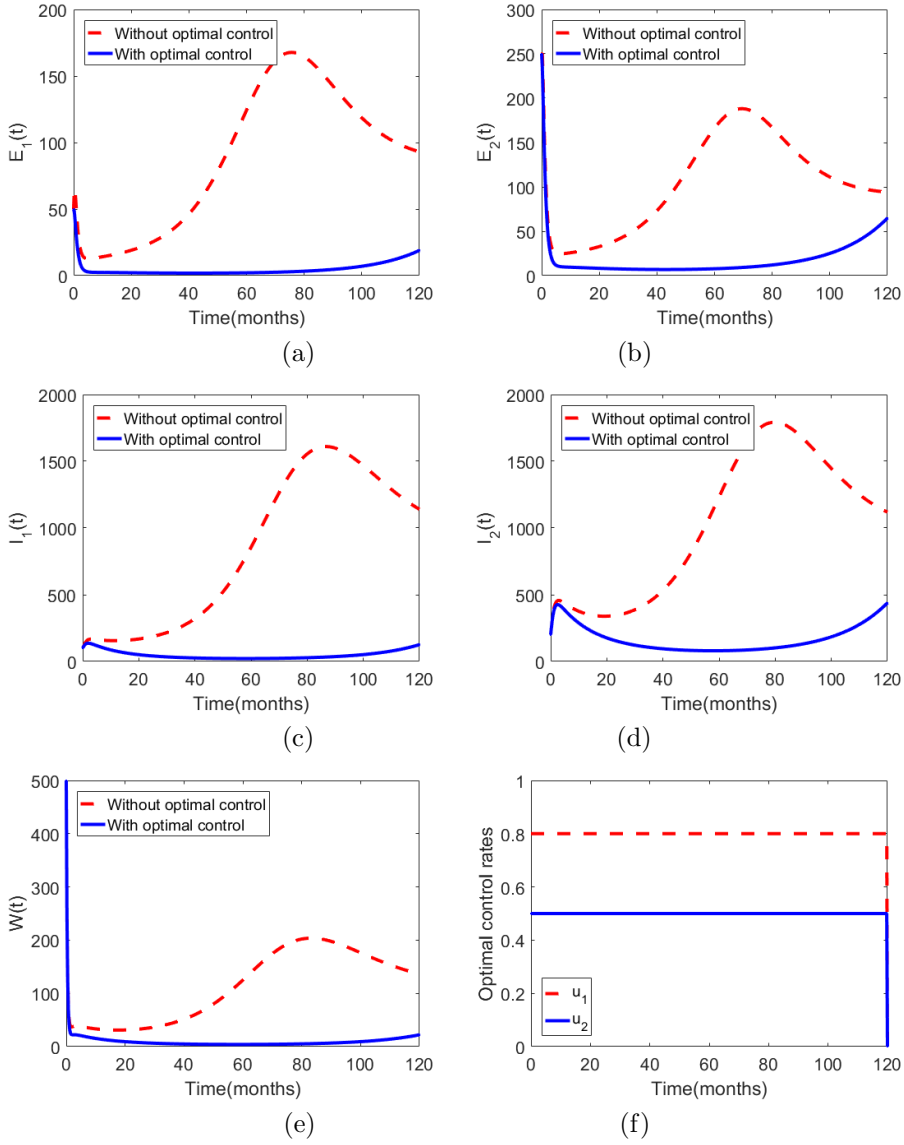

FIGURE 7. Solution of the model (asymptomatic individuals) with and without optimal control under heterogeneous setting, with $0 \leq u_1(t) \leq 0.8$ and $0 \leq u_2(t) \leq 0.5$.

Numerical results in Figure 8 suggest that when the cost of implementing the strategies is low B_i and the efforts are high A_i, then the disease can be effectively manage with control profiles at low intensity.

Simulation results in Figure 9 depicts the impact of varying the weights. In particular, we varied the weights A_i, while B_i, $i = 1, 2$, is fixed to $B_i = 10^{-2}$. As we can observe, increasing A_i may lead to varying optimal controls. Precisely, we can note that for value of A_1 greater that 10, the control profile for u_1 may not

TABLE 4. Summary of variations in the weight parameters and their corresponding effects, we set $\beta_2 = 1.5\beta_1$, with $\beta_1 = 3.6 \times 10^{-4}$, $0 \le u_1 \le 0.8$, $0 \le u_2 \le 0.5$. The initial population levels were assumed as follows, $S_1(0) = 1000$, $E_1(0) = 50$, $I_1(0) = 100$, $S_2(0) = 1200$, $E_1(0) = 250$, $I_1(0) = 200$ and $W = 500$.

A_1	A_2	B_1	B_2	Total cost J	New infections T_n
1	1	10	10	3.254×10^3	1.6731×10^3
2	2	10	10	5.9743×10^3	1.6731×10^3
1	1	10^2	10^2	8.0461×10^3	1.7086×10^3
2	2	10^2	10^2	1.0772×10^4	1.6874×10^3
2	2	10^3	10^3	5.8477×10^4	1.8044×10^3
5	5	10^3	10^3	6.6785×10^4	1.7393×10^3

need to be maintained at its maximum (0.8). However, in contrast we can note that the control profile for u_2 may not need to be maintained at its maximum (0.5) whenever A_2 is greater than 10^4. In a nutshell, one can conclude that whenever the control efforts are high and the cost of implementation is low, then the disease can be effectively controlled with control at varying and low intensity.

4. Conclusions

In this article, a differential equation-based two-patch model for guinea worm disease, a water-borne infection, is proposed and analysed. The proposed model is is concerned with different host populations at the two patches, but with a common water source. Results obtained from the study demonstrate that, while each patch could contribute differently to the infection risk and the transmission dynamics, the overall reproduction number is determined by the sum of the two individual reproduction numbers. Further, analytical and numerical results of the study show that this overall reproduction number, $\mathbb{R}_0$, can provide a sharp threshold for the disease dynamics: when $\mathbb{R}_0 \le 1$, the disease-free equilibrium is globally asymptotically stable, indicating that the infection would die out; when $\mathbb{R}_0 > 1$, there exists a unique endemic equilibrium which is globally asymptotically stable, and the disease persists.

Subsequently, we have performed an optimal control study on this two-patch model to effectively design control strategies for guinea worm disease. The main goal here, is to strengthen the efforts of educational campaigns so as to reduce the number of infectious human populations with minimal costs. From the analysis of the optimal control system observed that when the two patches have similar characteristics in disease transmission and control efforts, then the disease patterns will be same for the two patches. The reverse is true when the two patches have different disease characteristics. We also observed that the presence of optimal control will always be associated with lower total number of new infections compared to when there is no optimal control. However, the success of optimal control hinges on the total cost of implementing the strategies as well as its maximum strength. Furthermore, we observed that an increase in weight constants may lead to a remarkable increase on the total number of new infections.

Our study is not exhaustive and in future will consider the effects of combining educational campaigns with other control measures for guinea worm disease,

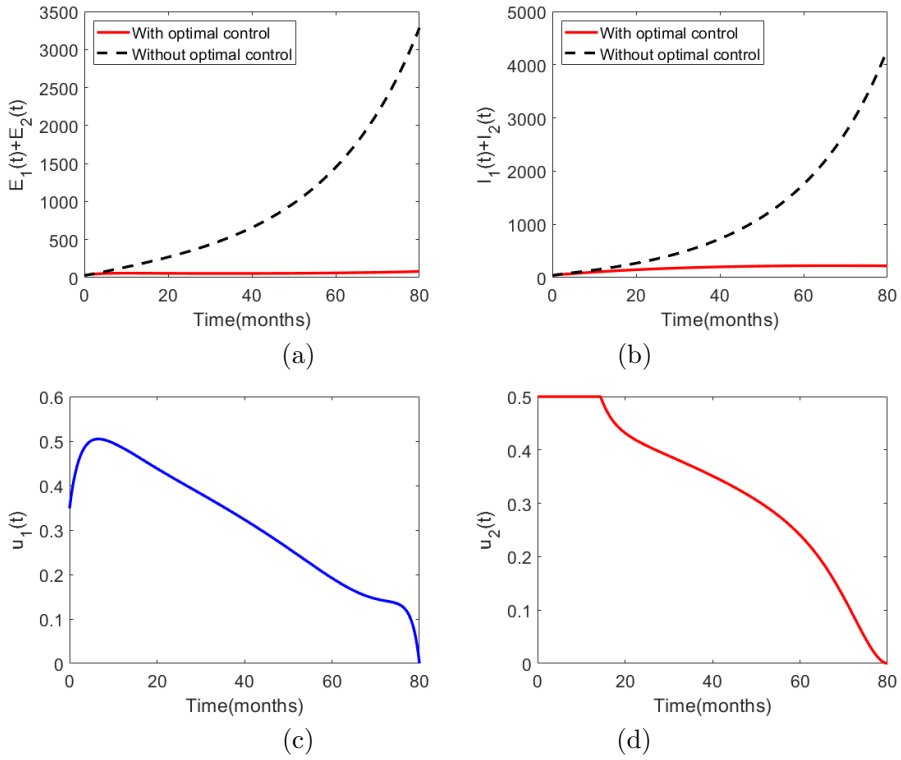

FIGURE 8. Simulation results for model system (2.1) with and without optimal control. We set $0 \leq u_1 \leq 0.8$, $0 \leq u_2 \leq 0.5$, $A_i = 100$ while B_i is fixed to 10^{-2}, and the rest of the parameters are as in Table 1. The solid curves in (a)-(b) represent the population levels of the host in the presence of optimal control while the dotted lines depict the population levels without optimal control. Figure (c) and (d) shows the control profiles.

such as water filter, larvicides, and surgery, in our optimal control study. These control methods, whether individually applied or combined together, might yield very different results with regard to the optimal control. Nevertheless, our findings illustrate that a strategic design of prevention and intervention methods for guinea worm disease that takes into account the unique setting of each different place may achieve the best outcome.

Acknowledgments. The authors would like to thank the anonymous referee and the handling editor Professor S. Lenhart for their suggestions that have improved this article.

REFERENCES

[1] Adetunde, I. A.; The Epidemiology of guinea worm infection in Tamale District, in the Northern Region of Ghana. *Journalof Modern Mathematics and Statistics*, (2008), 50-54.

[2] Alew, O. O., Peters, N.; Ethiopian Dracunculiasis Eradication Program (EDEP) GOG WOREDA. Meeting, National Review; 14-15 December 2015; Gambella, Ethiopia: 2015.

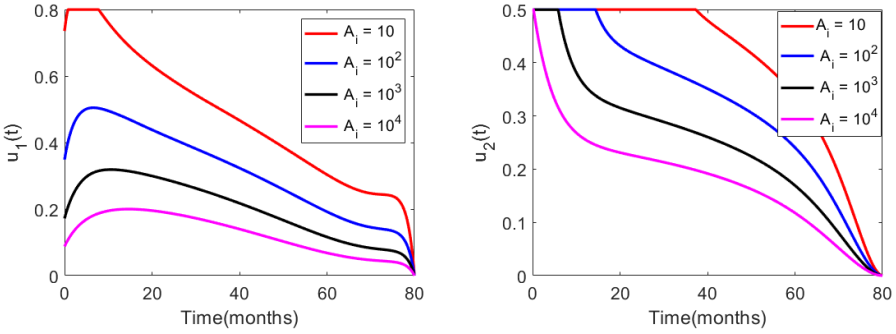

FIGURE 9. Simulation results for model system (2.1) illustrating the effects of varying the weights. We set $0 \leq u_1 \leq 0.8$, $0 \leq u_2 \leq 0.5$, and varied A_i while B_i is fixed to 10^{-2}, and the rest of the parameters are as in Table 1.

[3] Beyene, H. B.; Bekele, A; Shifara, A; Ebstie, Y. A.; Desalegn, Z; Kebede, Z; et al. Elimination of Guinea worm disease in Ethiopia; current status of the Disease's, eradication strategies and challenges to the end game. *Ethiop Med J*, **55**(Suppl 1), (2017), 15-31.

[4] Biswas, G.; Sankara, D. P.; Agua-Agum, J.; Maiga, A.; Dracunculiasis (guinea worm disease): Eradication without a drug or a vaccine. *Philos. Trans. R. Soc. B*, **368**, (2013), 20120146.

[5] Bhunu, C. P.; Mushayabasa, S.; Kojouharov, H.; Tchuenche, J. M.; Mathematical Analysis of an HIV/AIDS Model: Impact of Educational Programs and Abstinence in Sub-Saharan Africa, *J. Math. Model. Algorithms*, **10** (2011), 31-55.

[6] Cheesbrough, M.; Curtis, S.; District laboratory practice in tropical countries. second. Vol. **53**, Journal of Chemical Information and Modeling. Cambridge: Cambrige University press, (2013), 1689-1699.

[7] Cyclops an intermediate host for guinea worm. http: //www.who.int/water_health/resources/vector324 to 336.pdf Accessed May 25, 2013.

[8] Eisenberg, M. C.; Shuai. Z.; Tien, J. H.; van den Driessche, P.; A cholera model in a patchy environment with water and human movement, *Math. Biosci.* **246** (2013), 105-112.

[9] https://water.org/our-impact/ethiopia/. Accessed 31 December 2018.

[10] Fister, K. R.; Lenhart, S.; McNally, J. S.; Optimizing chemotherapy in an HIV model, *Electron. J. Differ. Equ.* textbf1998 no. 32 (1998), 1-12.

[11] Freedman, H. I.; Ruan, S.; Tang, M.; Uniform persistence and flows near a closed positively invariant set, *J. Dyn. Differ. Equat.* **6** (1994), 583-600.

[12] Hopkins, D. R.; Ruiz-Tiben, E.; Ruebush, T. K.; Diallo, N.; Agle, A.; Withers, C. J.; Dracunculiasis eradication: delayed, not denied. *Am. J. Trop. Med. Hyg*, **62** (2000), 163- 168

[13] Ilegbodu, V. A.; Kale, O. O.; Wise, R. A.; Christensen, B. L.; Steele, J. H.; Chambers, L. A.; Impact of guinea worm disease on children in Nigeria. The American Journal of Tropical Medicine and Hygiene, 35(5) (1986), 962-964.

[14] Joshi, H. R.; Lenhart, S.; Hota, S.; Agusto, F.; Optimal control of an SIR model with changing behavior through an education campaign, *Electron. J. Diff. Equ*, **2015** no. 50 (2015), 1-4.

[15] Lenhart, S.; Workman, J. T.; *Optimal Control Applied to Biological Models*, Chapman and Hall, 2007.

[16] Li, M. Y.; Graef, J. R.; Wang, L.; Karsai. J.; Global dynamics of a SEIR model with varying total population size, *Math. Biosci.* **160** (1999), 191-213.

[17] Link, K.; Guinea worm disease (Dracunculiasis): opening a mathematical can of worms. M.Sc. Thesis, Pennsylvania, USA, 2012.

[18] Losio, A. E.; Mushayabasa, S.; Modeling the effects of spatial heterogeneity and seasonality on guinea worm disease transmission, *Journal of Applied Mathematics*, **2018** (2018), Article ID 5084687, 12 pages.

[19] Lolika, O. P.; Modnak, C.; Mushayabasa, S.; On the dynamics of brucellosis infection in bison population with vertical transmission and culling, *Math. Biosci*, **305** (2018), 42-54.
[20] LaSalle, J. S.; *The stability of Dynamical Systems. CBMS-NSF Regional Conference Series in Applied Mathematics*, SIAM: Philadelphia, **25** (1976),
[21] Lukes, D. L.; Differential Equations: Classical to Controlled, Mathematics in Science and Engineering, Academic Press, New York, NY, USA, 1982.
[22] Lutambi, A.; Penny, M.; Smith, T.; Chitnis, N.; Mathematical modelling of mosquito dispersal in a heterogeneous environment, *Math. Biosci*, **214** (2013), 198-216.
[23] Mari, L; Ciddio, M; Casagrandi, R; Perez-Saez, J; Bertuzzo, E; Rinaldo, A; et al.; Heterogeneity in schistosomiasis transmission dynamics, emphJ. Theor. Biol, **432**, (2017), 87-99.
[24] Molyneux, D.; Sankara, D. P.; Guinea worm eradication: Progress and challenges-should we beware of the dog? *PLoS Negl. Trop. Dis*, **11**, (2017), e0005495.
[25] Mushayabasa, S.; Bhunu, C. P.; Smith?, R. J.; Assessing the impact of educational campaigns on controlling HCV among women in prison settings, *Commun. Nonlinear. Sci. Numer. Simul*, **17** (2011), 1714-1724.
[26] Netshikweta, R; Garira, W.; A Multiscale Model for the World's First Parasitic Disease Targeted for Eradication: Guinea Worm Disease, *Comput. Math. Methods. Med.*, **2017** (2017), 1473287.
[27] Pantha, B.; Day, J.; Lenhart, S.; Optimal control applied in an Anthrax epizootic model, *J. Biol. Syst.*, **24** (2016), 495-517.
[28] Pontryagin, L. S.; Boltyanskii, V. G.; Gamkrelidze, R. V.; Mishchenko, E. F.; The mathematical theory of optimal processes. Wiley, New Jersey, 1962.
[29] Samanta, S.; Rana, S.; Sharma, A; Misra, A. K.; Chattopadhyay, J.; Effect of awareness programs by media on the epidemic outbreaks: A mathematical model, *Appl. Math. Comp*, **219** (2013), 6965-6977.
[30] Sharma, A.; Misra, A. K.; Modeling the impact of awareness created by media campaigns on vaccination coverage in a variable population, *J. Biol. Syst*, **22** (2014), 249-270.
[31] Smith, R. J.; Cloutier, P.; Harrison, J.; Desforges, A.; A Mathematical Model for the eradication of guinea worm disease. Understanding the dynamics of emerging and re-emerging infectious diseases using mathematical models, 2012: 133-156.
[32] van den Driessche, P.; Watmough, J.; Reproduction numbers and sub-threshold endemic equilibria for compartmental models of disease transmission, *Math. Biosci.*, **180** (2002), 29-48.

Steady Mushayabasa (corresponding author)
Department of Mathematics, University of Zimbabwe, P.O. Box MP 167, Harare, Zimbabwe
Email address: steadymushaya@gmail.com

Anthony A. E. Losio
Department of Mathematics, University of Zimbabwe, P.O. Box MP 167, Harare, Zimbabwe
Email address: abulelosio@yahoo.com

Chairat Modnak
Department of Mathematics, Faculty of Science, Naresuan University, Phitsanulok 65000, Thailand
Email address: cmodn001@odu.edu

Jin Wang
Department of Mathematics, University of Tennessee at Chattanooga, 615 McCallie Ave., Chattanooga, TN 37403, USA
Email address: Jin-Wang02@utc.edu